

AD-A046 438

WEAPONS RESEARCH ESTABLISHMENT SALISBURY (AUSTRALIA)
OPTICAL DESIGN OF ASPHERIC MIRRORS. (U)
MAR 77 G W MCQUISTAN

F/G 20/6

UNCLASSIFIED

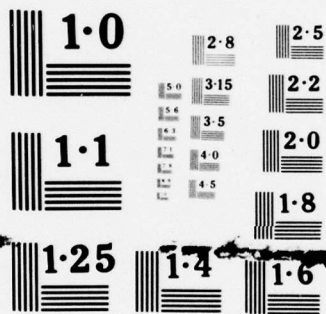
WRE-TR-1742(A)

NL

1 OF 1
ADA
046438



END
DATE
FILMED
12-77
DDC



NATIONAL BUREAU OF STANDARDS
MICROCOPY RESOLUTION TEST CHART



DEPARTMENT OF DEFENCE

DEFENCE SCIENCE AND TECHNOLOGY ORGANISATION

WEAPONS RESEARCH ESTABLISHMENT

SALISBURY, SOUTH AUSTRALIA

TECHNICAL REPORT 1742 (A)

OPTICAL DESIGN OF ASPHERIC MIRRORS

G.W. McQUISTAN

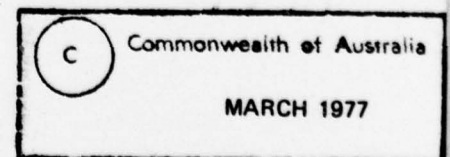


Approved for Public Release

AD No. —
DDC FILE COPY

COPY No. 5

DDC
RECEIVED
NOV 16 1977
A



APPROVED
FOR PUBLIC RELEASE

THE UNITED STATES NATIONAL
TECHNICAL INFORMATION SERVICE
IS AUTHORIZED TO
REPRODUCE AND SELL THIS REPORT

UNCLASSIFIED

AR-000-526

DEPARTMENT OF DEFENCE
DEFENCE SCIENCE AND TECHNOLOGY ORGANISATION
WEAPONS RESEARCH ESTABLISHMENT

9 TECHNICAL REPORT, 1742 (A)

6 OPTICAL DESIGN OF ASPHERIC MIRRORS. 11 Mar 77

10 G.W. McQuistan

12 25th

14 WRE-TR-1742(A)

S U M M A R Y

Aspheric mirrors have been designed for a number of infrared optical systems. The method developed to design these systems is described and illustrated by a number of particular cases.

Approved for Public Release

POSTAL ADDRESS: The Director, Weapons Research Establishment,
Box 2151, G.P.O., Adelaide, South Australia, 5001.

UNCLASSIFIED

371700

mac

DOCUMENT CONTROL DATA SHEET

Security classification of this page

UNCLASSIFIED

1	DOCUMENT NUMBERS	2	SECURITY CLASSIFICATION
AR Number: AR-000-526		a. Complete Document: Unclassified	
Report Number: WRE-TR-1742(A)		b. Title in Isolation: Unclassified	
Other Numbers:		c. Summary in Isolation: Unclassified	
3	TITLE		
OPTICAL DESIGN OF ASPHERIC MIRRORS			
4	PERSONAL AUTHOR(S):	5	DOCUMENT DATE:
G.W. McQuistan		March 1977	
		6	6.1 TOTAL NUMBER OF PAGES 25
		6.2 NUMBER OF REFERENCES: 5	
7	7.1 CORPORATE AUTHOR(S):	8	REFERENCE NUMBERS
Weapons Research Establishment		a. Task: DST 76/14	
7.2 DOCUMENT (WING) SERIES AND NUMBER Applied Physics Wing TR-1742		b. Sponsoring Agency: RD73	
9	COST CODE:		
308771			
10	IMPRINT (Publishing establishment):	11	COMPUTER PROGRAM(S) (Title(s) and language(s))
Weapons Research Establishment			
12	RELEASE LIMITATIONS (of the document):		
Approved for Public Release			
12.0	OVERSEAS	NO	P.R. 1 A B C D E

Security classification of this page:

UNCLASSIFIED

13 ANNOUNCEMENT LIMITATIONS (of the information on these pages):

No Limitation

14 DESCRIPTORS:

- | | | |
|---------------------------|---|--|
| a. EJC Thesaurus
Terms | Aspheric optics
Infrared optics
Optical design
Optical equipment | Design
Mirrors
Infrared optical
systems |
| b. Non-Thesaurus
Terms | | |

15 COSATI CODES:

2006
1705

16 LIBRARY LOCATION CODES (for libraries listed in the distribution):

SW SR SD AAC NL

17 SUMMARY OR ABSTRACT:

(if this is security classified, the announcement of this report will be similarly classified)

Aspheric mirrors have been designed for a number of infrared optical systems. The method developed to design these systems is described and illustrated by a number of particular cases.

TABLE OF CONTENTS

	Page No.
1. INTRODUCTION	1
2. DESIGN THEORY	1 - 3
3. COMPUTATION METHODS	3 - 5
3.1 Runge-Kutta integration	3 - 5
3.2 Curve fitting to the aspheric	5
3.3 Ray tracing through an aspheric defined by points	5
4. ACCURACY AND PERFORMANCE	5 - 6
5. CONCLUSIONS	6
REFERENCES	7

LIST OF APPENDICES

I RELATIONSHIP BETWEEN TWO CONGRUENCES IN A REFLECTING OPTICAL SYSTEM	8 - 9
II TEST SYSTEM (DOUBLE PARABOLA)	10
III SECTOR SCANNER SYSTEM	11 - 12
IV BOLOMETER RADIOMETER	13
TABLE 1. CURVE FITTING ERRORS	6

LIST OF FIGURES

1. Determination of aspheric surfaces
2. Congruence specifications
3. Accuracy of test parabola
4. Congruences at a reflecting surface
5. Double parabola
6. General arrangement of sector scanner aspherics
7. In going congruence sector scanner
8. Out going congruence sector scanner
9. Congruences bolometer radiometer

ACCOMMODATION FOR	
WFO	Write Section <input checked="" type="checkbox"/>
DDG	Draft Section <input type="checkbox"/>
UNANNOUNCED	<input type="checkbox"/>
JUSTIFICATION.....	
BY.....	
DISTRIBUTION/AVAILABILITY CODES	
Dist.	AVAIL. and SPECIAL
A	

1. INTRODUCTION

In the design of optical systems it is often convenient and efficient to make use of surfaces that are aspherical (i.e., not spherical). The use of aspheric surfaces has not been common practice because of the cost of producing such surfaces but with the development of numerically controlled machines capable of cutting metal surfaces to high accuracy this cost disadvantage has been somewhat reduced. Positional accuracy and finish available from diamond cut metals is still not so good as that required for optical systems using the visible wavelengths, but for systems using the longer wavelength of the infrared part of the spectrum (10 to 20 times longer than visible light), presently available accuracies are adequate.

Aspheric surfaces are useful in optical systems in a number of ways. However, it should firstly be stressed that these surfaces are not capable of solving all the optical designer's problems. Aspheric elements, either mirrors or lenses, have been used for many years in light concentrating systems and illuminators. Such systems have not required high aberration correction and adequate performance has been obtained with relatively simply produced elements. Astronomical telescopes have also for many years employed aspheric elements but the manufacture of these has been a process of repeated grinding, polishing and testing. In more recent years aspheric elements have been used in a large variety of systems particularly in high aperture systems and catadioptric systems where good aberration correction is required over large fields of view.

In general infrared systems require optics that have relatively large apertures and large focal ratios. Also because fewer materials with suitable transmission properties and refractive indices are available in the infrared part of the spectrum as compared to the visible, reflecting elements are more desirable. For systems with only small fields of view purely reflecting systems are practical, when the above restrictions are considered, but for large fields of view at least some refracting elements have to be employed.

The methods of design described in this paper reflect a build up in facilities to assess designs and to produce actual aspheric surfaces. Initially it was the aim to produce both designs and surfaces that could be described by an even order polynomial of ten terms (i.e., up to terms of 20th power of radial distance). However, as limitations of this aim became apparent the facilities were modified so that aspheric curves, expressed by points and gradients, could be assessed by ray tracing and manufactured directly from this information.

2. DESIGN THEORY

The method of design employed for the aspheric mirrors differs from the traditional method of considering aberrations. It involves consideration of the basic optical invariants of the systems. The systems are designed to be aplanatic, that is, the on-axis image must be formed by rays that are:

- (1) perfectly stigmatic (all pass through the one point)
- (2) obey the sine condition (the relationship between the angles of rays to the axis in image and object space).

These above two conditions are the ones that are employed in the actual design of the systems as is shown below. In terms of traditional aberration these two conditions make the two Seidel aberrations, spherical aberration and coma, both equal to zero.

To image an object in such a manner as to fulfill the two conditions stated above, two reflecting surfaces are required and these can in general be placed in any position. Having specified the positions of the object, image and the two optical surfaces the shapes of the surfaces are then implicitly defined. The problem is then to determine these surfaces in suitable explicit forms.

Before giving details of how this is done it is necessary to indicate the more general problem that has to be solved. It is necessary in many optical systems to have more than two elements and this is particularly so with reflecting systems where large obscurations have to be avoided. Further it is inconvenient and still costly to have large aspheric surfaces. It can be shown that two aspheric surfaces can be used in combination with any number of other surfaces, both spherical and aspheric, to produce an aplanatic system(ref.1). With only one aspheric surface, in general, it is possible to correct only on-axis aberrations. Consider an optical system (shown schematically in figure 1) imaging a source S to an image at I by a series of optical surfaces. Aspheric surfaces can be introduced at A and B to make the system aplanatic or surfaces already at these positions can be modified to produce the same result. There is no restriction requiring the two aspheric surfaces to be adjacent. They may be separated by other surfaces. Both these situations can be dealt with by the method described below. When surfaces other than the aspherics are present the aspherics correct the coma and spherical aberration of these other surfaces. Thus to determine the aspherics the aberration contributions of the other surfaces must be specified in some manner.

The rays from the on-axis source in object space, pass through the various optical surfaces and form a normal rectilinear congruence at A. Each ray (R_i) passing through the plane normal to the axis at A can be described by a relationship of the form

$$y = h_i + x \cdot \tan \omega_i \quad (1)$$

It is the relationship between the values of h_i and ω_i that describe the congruence and this relationship depends upon the aberrations of the previous surfaces.

In a similar manner the rays (R'_i) from the image I, can be traced back through the system and described by a relationship similar to equation (1) where they intersect the normal plane at B. Here they form another normal rectilinear congruence which contains implicitly the aberrations of the surfaces between B and I.

These congruences, that is the relationships between the values of h and ω , can be expressed either as an explicit mathematical relationship, or an implicit one through parameters, or in tabular form. Explicit relationships are used throughout this paper. The various methods of specifying the values are shown in figure 2, where (a) is typical of a system with an element before the aspheric and (b) with one following. Parameters t and t' are to be used as the independent variables in the differential equations with one being eliminated in terms of the other. Here these are always defined by the relationships (2), but any parameters would be suitable which provides a relationship between θ and θ' .

$$t = \sin \theta \text{ and } t' = \sin \theta' \quad (2)$$

Then ω and ω' must be expressed in terms of t and t' , respectively. It is obvious that the sine condition is a linear relation between t and t' . Figure 2(c) illustrates the point that the source or the image may be at infinity and then $\omega = 0$ and $t = h$. These definitions are further illustrated by the examples in the appendices.

Having established the two congruences of rays, the corresponding member rays of each congruence may be connected by a single intermediate ray following the simple rules of reflection and refraction. (The details are provided in Appendix I).

In Appendix I the relationship between two congruences in a reflecting optical system are deduced. These are expressed in equations (I.6) and (I.7) from that Appendix, repeated here

$$\frac{dx}{dt} = - \left[\frac{R \cos \omega - R_x}{R \sin \omega - R_y} + \tan \omega \right]^{-1} \left[\frac{dh}{dt} + x \frac{d}{dt} (\tan \omega) \right] \quad (3)$$

$$\frac{dx'}{dt} = - \left[\frac{R \cos \omega' - R_x}{R \sin \omega' - R_y} + \tan \omega' \right]^{-1} \left[\frac{dh'}{dt} + x' \frac{d}{dt} (\tan \omega') \right] \quad (4)$$

where

$$R_y = y' - y, R_x = x' - x \text{ and } R = (R_x^2 + R_y^2)^{\frac{1}{2}} \quad (5)$$

These above two partial differential equations when solved simultaneously provide uniquely the two surfaces which will make the optical system aplanatic. The last bracketed term of each differential equation contains the terms involving the aberrations for the congruences and the explicit relations are shown in the various Appendices (II to IV) where a number of examples are shown.

3. COMPUTATION METHODS

In this section the more unusual aspects of the calculations are described, but it is not intended to be a complete description of the mathematical method.

In dealing with aspheric surfaces there is a difficulty as to how best to define a particular surface. In the present instance two definitions have been used. Firstly, the aspheric surfaces are defined as series of points on the surfaces. While this is the most accurate method of defining the surfaces it is a very inconvenient definition with which to perform procedures such as ray tracing. To overcome this problem a second method of definition is also used. That is the aspheric surface is defined as a polynomial of the form

$$x = \sum_{i=1}^{10} A_i y^{2i} \quad (6)$$

Equation (6) is to be considered as an approximation to the basic point definition and is used in the various procedures employed to obtain an initial approximate solution from which the true solution is found using the point definition.

3.1 Runge-Kutta integration

The Runge-Kutta integration is employed to integrate the pair of simultaneous differential equations (3) and (4). The particular method used is based on one given by Piaggio(ref.2). If the pair of differential equations are

$$\frac{dx}{dt} = F(t, x, x') \quad (7)$$

and

$$\frac{dx'}{dt} = G(t, x, x') \quad (8)$$

then

$$\left. \begin{aligned} k^i &= \delta h \cdot F(t_o, x_o, x'_o) \\ l^i &= \delta h \cdot G(t_o, x_o, x'_o) \end{aligned} \right\} \quad (9)$$

and

$$\left. \begin{aligned} k^{ii} &= \delta h \cdot F(t_o + \delta h/3, x_o + k^i/3, x'_o + l^i/3) \\ l^{ii} &= \delta h \cdot G(t_o + \delta h/3, x_o + k^i/3, x'_o + l^i/3) \end{aligned} \right\} \quad (10)$$

and

$$\left. \begin{aligned} k^{iii} &= \delta h \cdot F(t_o + 2\delta h/3, x_o + k^{ii} - k^i/3, x'_o + l^{ii} - l^i/3) \\ l^{iii} &= \delta h \cdot G(t_o + 2\delta h/3, x_o + k^{ii} - k^i/3, x'_o + l^{ii} - l^i/3) \end{aligned} \right\} \quad (11)$$

and

$$\left. \begin{aligned} k^{iv} &= \delta h \cdot F(t_o + h, x_o + k^{iii} - k^{ii} + k^i, x'_o + l^{iii} - l^{ii} + l^i) \\ l^{iv} &= \delta h \cdot G(t_o + h, x_o + k^{iii} - k^{ii} + k^i, x'_o + l^{iii} - l^{ii} + l^i) \end{aligned} \right\} \quad (12)$$

then

$$\left. \begin{aligned} x_o(N+1) &= x_o(N) + (k^i + 3k^{ii} + 3k^{iii} + k^{iv})/8 \\ x_o^i(N+1) &= x'_o(N) + (l^i + 3l^{ii} + 3l^{iii} + l^{iv})/8 \end{aligned} \right\} \quad (13)$$

This integration system has been tested in a number of ways with differential equations that are likely to be encountered in defining aspheric surfaces. All tests have shown sufficient accuracy is obtainable, however, it is possible that in certain circumstances (i.e., with very complex curves) the integration system could become inaccurate.

In general 600 points have been used but tests with half this number and with δh doubled have produced identical results.

3.2 Curve fitting to the aspheric

It is necessary to determine the ten coefficients (A_1) of equation (6) so that this equation gives a good fit to the actual points on the aspheric surface and also that the slopes (gradients) of the aspheric surface are accurately followed. This last point is important because the accuracy of the gradients can have a marked effect upon procedures such as ray tracing.

To fit the curve to the original points, twenty of these original points are selected with a density distribution along the radius (R_0) proportional to $\sin(R/2R_0)$. This gives more weight to the periphery of the surface roughly in proportion to the area. The central curvatures of the surfaces can be calculated either by the Gaussian optical approximation or using points of the original set close to the vertex. In practice the third point (second from the vertex) of the 600 has been used and found to give satisfactory results. The slopes at the twenty selected points are found from the angles between the appropriate in going and outgoing rays to the aspheric surface, these rays being defined, one by the appropriate congruence and the other by the line joining the corresponding points on the two aspherics. Using the twenty points and twenty slopes, together with the central curvature, the ten coefficients of the even order polynomial describing the surface are found by a method of least squares.

3.3 Ray tracing through an aspheric defined by points

Existing computer programs were available to provide ray traces through surfaces defined by explicit mathematical relationships. Using such a program and the fitted curve an approximate intersection was found. A correction to the point of intersection was then calculated by interpolating the curve and the slope. The procedure was continued until the correction became insignificant. (See for example Welford(ref.3)).

Newton's method of divided differences was used to provide the interpolation. Five adjacent original points in the region of the intersection were used, which in effect defines a fourth degree polynomial to the aspheric curve in that region. Because of the differencing it was found necessary to employ double precision in this section of the program.

As with all ray tracing programs extreme cases can be found that this program is incapable of dealing with. In particular when using aspherics in optical systems with small focal ratios (less than $F/0.6$) rays that travel nearly normal to the direction of the optical axis may be found that will not be handled by the program.

4. ACCURACY AND PERFORMANCE

As has already been pointed out the Runge-Kutta integration system has been tested with a number of points and intervals and consistent results were obtained within a few parts in 10^{10} .

For a further check on the accuracy an optical system was designed (see Appendix II) in which two mirrors were used to image a source in a symmetrical arrangement. The solution was, of course, two identical parabolas. The error in the determination of these curves is given in figure 3.

To test the curve fitting subroutines the system as shown in Appendix III was run at a number of different apertures. This system has a 6 inch radius spherical mirror as the first element and the aspherics are required to correct the spherical aberration from this mirror. With apertures up to 8 inches in diameter it is to be expected that the aspherics would be complex and therefore difficult to represent accurately by a polynomial. Table 1 below gives the curve fitting errors for three diameters.

TABLE 1. CURVE FITTING ERRORS

Aperture diameter	r.m.s. curve error	Maximum curve error	r.m.s. gradient error
4 inches	6×10^{-8} inches	10^{-7} inches	9×10^{-8}
6 inches	1.8×10^{-6} inches	3×10^{-6} inches	1×10^{-5}
8 inches	1.8×10^{-3} inches	2.8×10^{-3} inches	2.4×10^{-2}

These figures indicate that for a 4 inch and 6 inch aperture system of this type the polynomial approximation is satisfactory and could have been used for ray tracing. However, beyond 6 inches the errors become large very quickly and the polynomial is useful only as a first approximation. A similar situation exists with all systems with significant errors appearing when large apertures are used or many combinations of aberrations require correction.

In Appendix IV the differential equations are deduced for a bolometer radio-meter (two mirror telescope). Both this system and that of Appendix II are two mirror systems without other aberration contributing optical elements. The aspheric surfaces for such systems can be determined explicitly by other methods. For example Head(ref.5) gives a method applicable to two mirror aplanatic systems. However, the advantage of the method described in this report is its ability to include additional optical elements that introduce aberrations whether they be of significant optical power or flat windows such as might be used to encapsulate a bolometer.

5. CONCLUSIONS

A method of designing aspheric mirrors has been outlined which has been tested and found to provide reliable results. The method is intended to be used in optical systems to correct on-axis aberrations and produce aplanatic systems. A selection of systems that have been designed is included in the Appendices II, III and IV to illustrate the application of the design method.

REFERENCES

No.	Author	Title
1	Born, M. and Wolf, E.	"Principles of Optics". (2nd Revised Edition 1964) Section 4.10
2	Piaggio, H.T.H.	"Differential Equations". Bell 1944
3	Welford, W.T.	"Aberrations of the Symmetrical Optical System". Academic Press 1974
4	Wasserman, G.D. and Wolf, E.	"On the Theory of Aplanatic Aspheric Systems". Proc. Phys. Soc. (London) 62, 2, 1949
5	Head, A.K.	"The Two-Mirror Aplanat". Proc. Phys. Soc. (London) 70, 945, 1957

APPENDIX I

RELATIONSHIP BETWEEN TWO CONGRUENCES IN A REFLECTING OPTICAL SYSTEM

Let a congruence be defined by a set of rays one of which is specified by (h, ω) . This ray meets the surface at P (see figure 4) and is reflected back to cut the X-axis at an angle ω^* . Let the plane tangent to the surface at P make an angle θ with the X-axis.

Then

$$\theta = \omega + \frac{\pi}{2} + a_1 \quad \text{or} \quad a_1 = \theta - \omega - \frac{\pi}{2} \quad (I.1)$$

and

$$\theta = \omega^* + \frac{\pi}{2} - a_2 \quad \text{or} \quad a_2 = -\theta + \omega^* + \frac{\pi}{2} \quad (I.2)$$

From Snell's law for reflecting surfaces

$$\sin a_1 = -\sin a_2$$

therefore

$$\cos(\omega - \theta) = \cos(\omega^* - \theta)$$

and

$$\cos \omega \cos \theta + \sin \omega \sin \theta = \cos \omega^* \cos \theta + \sin \omega^* \sin \theta \quad (I.3)$$

Let the surface be expressed in a parametric form with 't' as the parameter, then

$$\frac{dy}{dx} = \tan \theta, \quad \text{and} \quad \cos \theta = \frac{dx}{dt}, \quad \text{and} \quad \sin \theta = \frac{dy}{dt},$$

thus equation (I.3) can be written

$$\frac{dx}{dt} \left[\frac{\cos \omega - \cos \omega^*}{\sin \omega - \sin \omega^*} \right] = - \frac{dy}{dt} \quad (I.4)$$

Now expressing the surface in terms of the congruence, the x and y coordinates satisfy

$$y = h + x \tan \omega$$

and equation (I.4) gives

$$\frac{dx}{dt} \left[\frac{\cos \omega - \cos \omega^*}{\sin \omega - \sin \omega^*} \right] = - \left[\frac{dh}{dt} + x \frac{d}{dt} (\tan \omega) + \tan \omega \frac{dx}{dt} \right] \quad (I.5)$$

which reduces to

$$\frac{dx}{dt} = - \left[\frac{\cos \omega - \cos \omega^*}{\sin \omega - \sin \omega^*} + \tan \omega \right]^{-1} \left[\frac{dh}{dt} + x \cdot \frac{d}{dt} (\tan \omega) \right] \quad (I.6)$$

Now if there are two congruences such as the one above, and another whose input ray is the output ray (ω^*) of the first, a further equation can be set up for this second congruence similar to the first. In this case the parameter t' is eliminated by using the relationship between t and t' (sine condition)

That is

$$\frac{dx'}{dt} = - \left[\frac{\cos \omega' - \cos \omega^*}{\sin \omega' - \sin \omega^*} + \tan \omega' \right]^{-1} \left[\frac{dh'}{dt} + x' \cdot \frac{d}{dt} (\tan \omega') \right] \quad (I.7)$$

From these it is possible to eliminate the ω^* by considering the relationship between P and the corresponding points (say Q) on the other congruence.

P has coordinates $(x, y) = (x, h + x \tan \omega)$.

Q has coordinates $(x', y') = (x', h' + x' \tan \omega')$.

Let

$$R_y = y' - y \text{ and } R_x = x' - x \text{ and } R = (R_x^2 + R_y^2)^{1/2} \quad (I.8)$$

then

$$\sin \omega^* = \frac{R_y}{R} \text{ and } \cos \omega^* = \frac{R_x}{R} \quad (I.9)$$

Thus equations (I.6) and (I.7) represent two partial differential equations which when solved simultaneously will provide a unique solution. This is based on a general method of solution described by Born and Wolf(ref.1) and Wasserman and Wolf(ref.4).

APPENDIX II

TEST SYSTEM (DOUBLE PARABOLA)

In this test system, which was used to check the accuracy of the computational system, a source at RA (see figure 5) is to be imaged at XF after reflection in aspheric surfaces at X2 and X3. The distances RA to X2 and X3 to XF were made equal. Apart from putting in numerical values of these distances this is the only information required.

Points on the aspherics

$$y' = h' + x' \tan \omega' \quad y = h + x \tan \omega \quad (\text{II.1})$$

A parameter t was chosen such that

$$t = \sin \omega \quad (\text{II.2})$$

To preserve the sine condition

$$t = \sin \omega = -\sin \omega' \quad (\text{II.3})$$

Also

$$h' = (X3 - XF) \tan \omega' \text{ and } h = (X2 - RA) \tan \omega \quad (\text{II.4})$$

Equations (II.4) are the congruences for each surface and equation (II.3) provides the relationship that must be held between them.

Using equations (I.6) and (I.7) of Appendix I, differential equations for the solution of this system are obtained as follows:

$$\frac{dx}{dt} = - \left[\frac{R_x - R \cos \omega}{R_y - R \sin \omega} + \tan \omega \right]^{-1} (X2 - RA + X) / \cos^3 \omega \quad (\text{II.5(a)})$$

$$\frac{dx'}{dt} = \left[\frac{R_x - R \cos \omega'}{R_y - R \sin \omega'} + \tan \omega' \right]^{-1} (X3 - XF + X') / \cos^3 \omega' \quad (\text{II.5(b)})$$

These are soluble in conjunction with the relations

$$R_y = y' - y, R_x = x' - x \text{ and } R = (R_x^2 + R_y^2)^{1/2} \quad (\text{II.6})$$

This system, as might be expected, results in two identical parabolas and the accuracy of their determination is discussed in the body of the paper.

It should be noted that the beams leaving the source and approaching the image are not aberrated and therefore the last bracketed term of the differential equations are of the form $(A + X) / \cos^3 \omega$.

APPENDIX III

SECTOR SCANNER SYSTEM

III.1 In going congruence

The positions of points on the surface (x,y) are expressed in terms of h and ω by

$$y = h + x \tan \omega \quad (\text{III.1})$$

From the geometry of the sphere (see figure 7)

$$t \approx R_o \sin \omega/2 \quad (\text{III.2})$$

and

$$h = \left(X_2 + \frac{R_o}{2 \cos \frac{\omega}{2}} \right) \tan \omega \quad (\text{III.3})$$

This last equation is the congruence relating h and ω for all rays and thus contains the aberrations of the sphere. Substituting this into equation (I.6) of Appendix I the first of the partial simultaneous differential equations is obtained

$$\begin{aligned} \frac{dx}{dt} = & - \left[\frac{R_x - R \cos \omega}{R_y - R \sin \omega} + \tan \omega \right]^{-1} R_o \frac{2}{\cos \frac{\omega}{2}} \left[\frac{1}{\cos^2 \frac{\omega}{2}} \left(X_2 + \frac{R_o}{2 \cos \frac{\omega}{2}} \right) \right. \\ & \left. + \tan \omega \left(\frac{R_o}{4} \frac{\tan \frac{\omega}{2}}{\cos \frac{\omega}{2}} + \frac{X}{\cos^2 \frac{\omega}{2}} \right) \right] \quad (\text{III.4}) \end{aligned}$$

Note the complexity of the last term now that aberrations are present in the input beam.

III.2 Outgoing congruence (see figure 8)

Again

$$y' = h' + x' \tan \omega' \quad (\text{III.5})$$

and

$$h' = (X_3 - XF) \tan \omega' \quad (\text{III.6})$$

and to maintain the sine condition

$$t/Ft = - \sin \omega' \quad (\text{III.7})$$

where $F\ell$ is the focal length.

Again, using equation (I.7) of Appendix I the second differential equation is obtained, namely

$$\frac{dx'}{dt} = \left[\frac{R_x - R \cos \omega'}{R_y - R \sin \omega'} + \tan \omega' \right]^{-1} \left[\frac{X_3 - XF + x'}{F\ell \cos^3 \omega'} \right] \quad (\text{III.8})$$

Equations (III.4) and (III.8) are solved simultaneously to define the two surfaces at X_2 and X_3 .

APPENDIX IV
BOLOMETER RADIOMETER

Object Space Congruence (see figure 9)

$$\left. \begin{aligned} \omega &= 0 \\ h &= t \end{aligned} \right\} \quad (IV.1)$$

Image Space Congruence

$$\left. \begin{aligned} \omega' &= -\theta \\ h' &= (XF - X3) \tan \theta \end{aligned} \right\} \quad (IV.2)$$

Let $t' = \sin \theta$, then to preserve the sine condition

$$t = f \sin \theta$$

Therefore

$$t = f t'$$

where f is the focal length. Equation (I.6) and (I.7) from Appendix I may be written as

$$\frac{dx}{dt} = - \left[\frac{R \cos \omega - R_x}{R \sin \omega - R_y} + \tan \omega \right]^{-1} \left(\frac{dh}{dt} + x \cdot \frac{d}{dt} \tan \omega \right) \quad (IV.3)$$

and

$$\frac{dx'}{dt} = - \left[\frac{R \cos \omega' - R_x}{R \sin \omega' - R_y} + \tan \omega' \right]^{-1} \left(\frac{dh'}{dt} + x' \cdot \frac{d}{dt} \tan \omega' \right) \quad (IV.4)$$

substituting from above

$$\frac{dx}{dt} = \left[\frac{(R - R_x)}{R_y} \right]^{-1} \quad (IV.5)$$

$$\frac{dx'}{dt} = - \left[\frac{R \cos \omega' - R_x}{R \sin \omega' - R_y} + \tan \omega' \right]^{-1} \frac{(XF - X3 - X')}{f \cos^3(\omega')} \quad (IV.6)$$

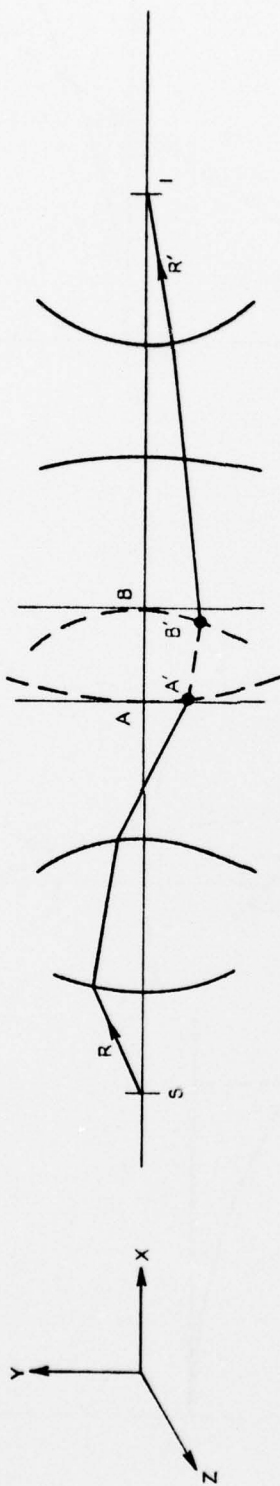


Figure 1. Determination of aspheric surfaces

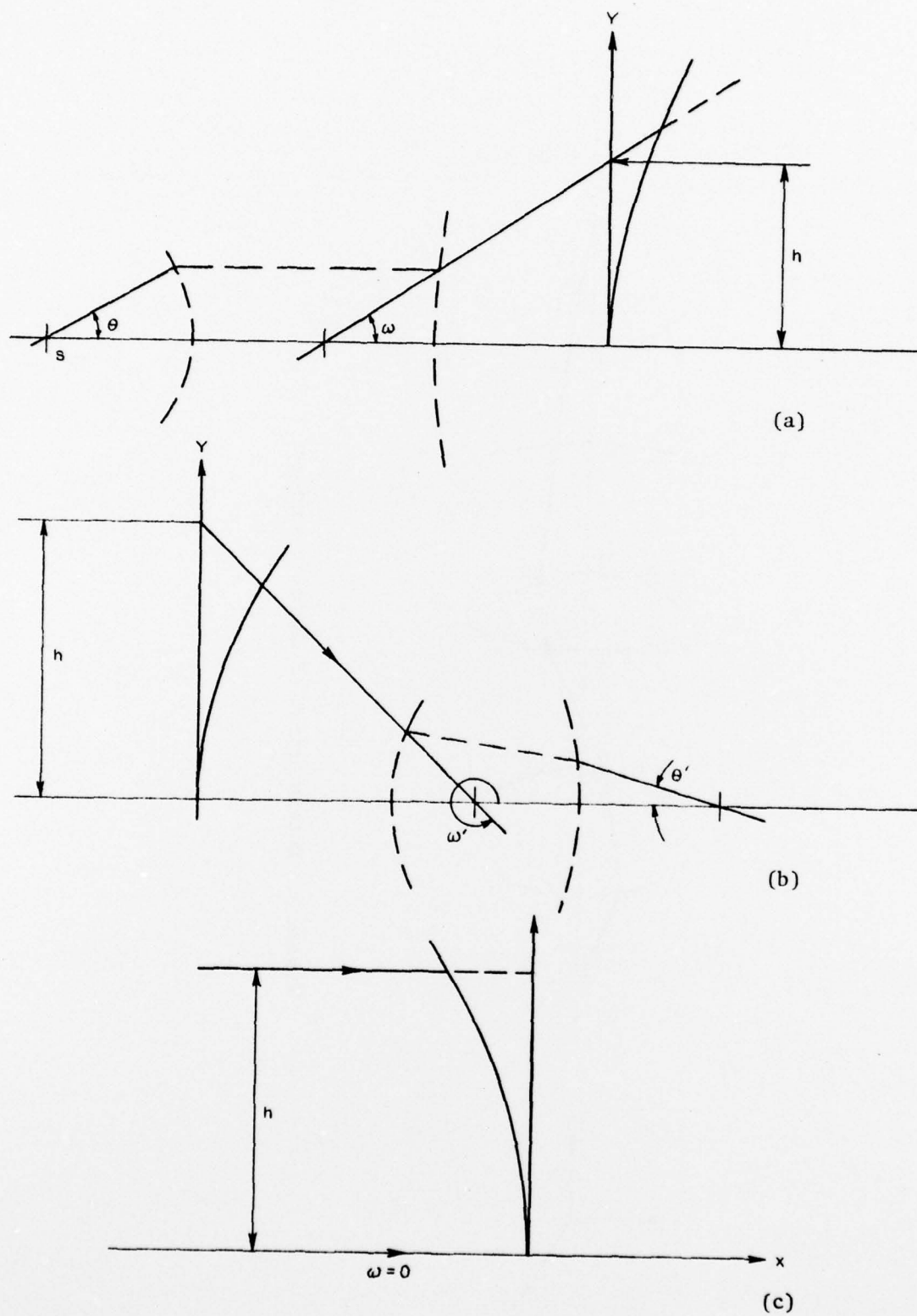
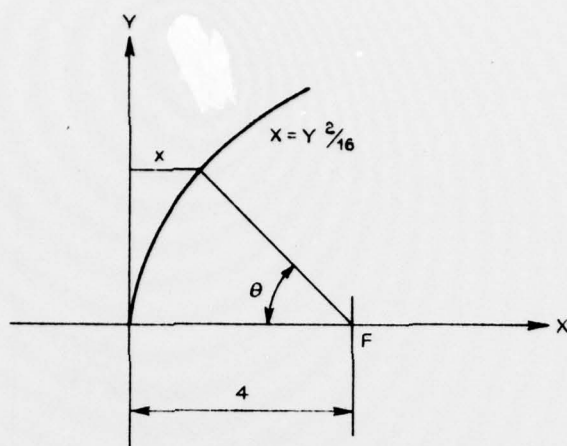


Figure 2. Congruence specifications



θ degrees	Δx
0.3	-5×10^{-11}
1.2	5×10^{-10}
5.5	5×10^{-8}
11.5	10^{-7}
17.5	3×10^{-7}
23.5	10^{-6}
30	-1.4×10^{-6}
37	2×10^{-6}
44.5	10^{-6}
53	10^{-5}

θ degrees	Δx
64	9×10^{-6}
72	6×10^{-6}
73.5	-1×10^{-6}
75	-2×10^{-6}
76	-3×10^{-6}
77	-5×10^{-6}
78.5	-1.3×10^{-5}
80	-4×10^{-5}
82	-2.1×10^{-4}
84.5	-2.9×10^{-3}

Figure 3. Accuracy of test parabola

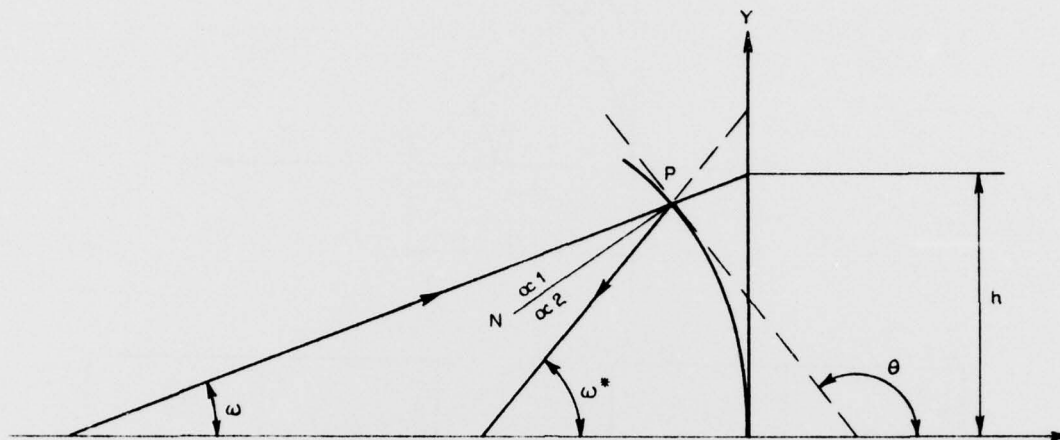


Figure 4. Congruences at a reflecting surface

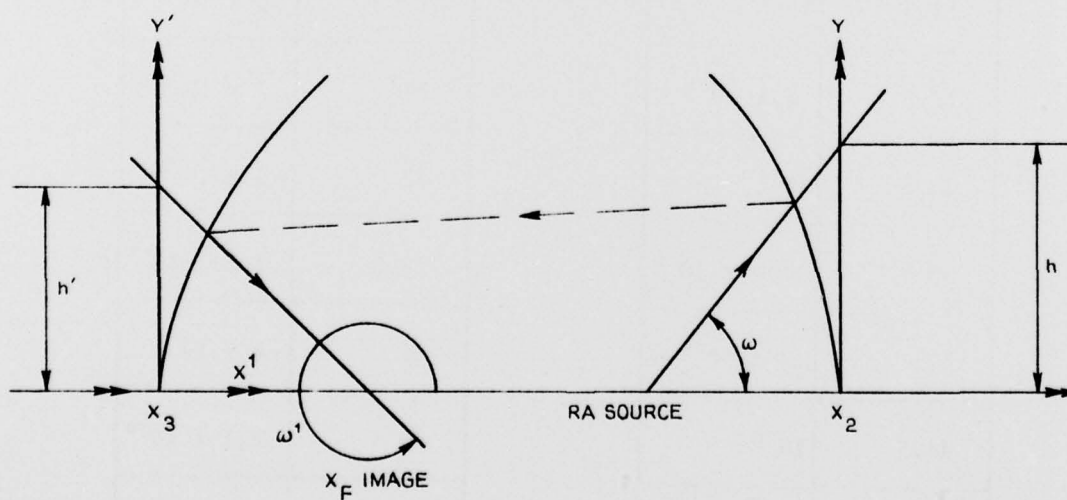


Figure 5. Double parabola

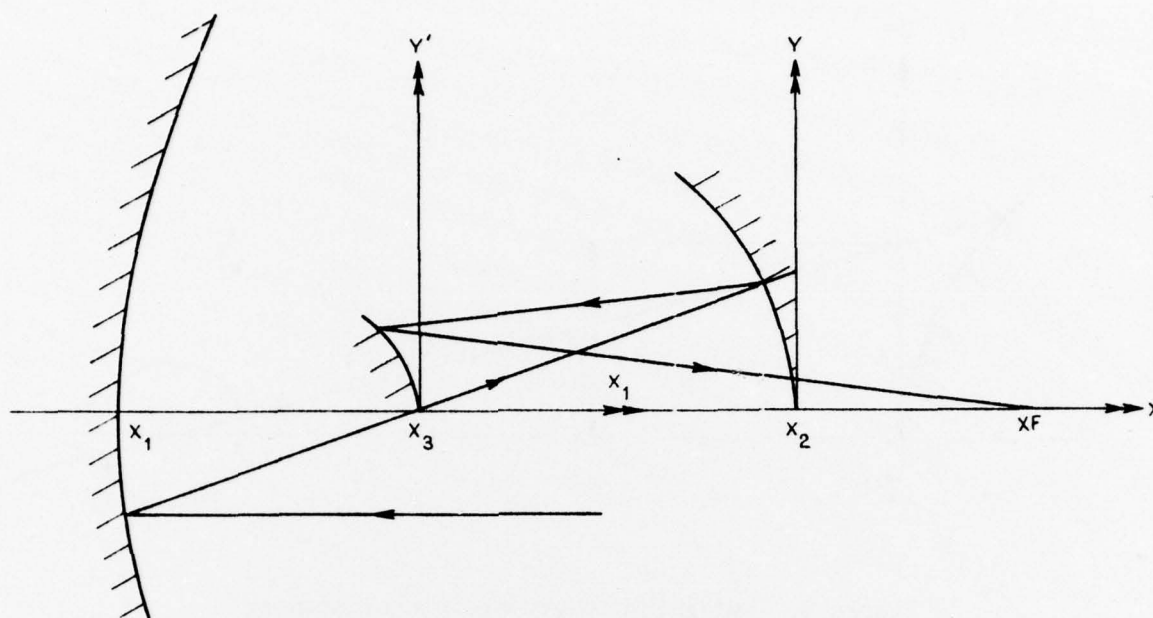


Figure 6. General arrangement of sector scanner aspherics

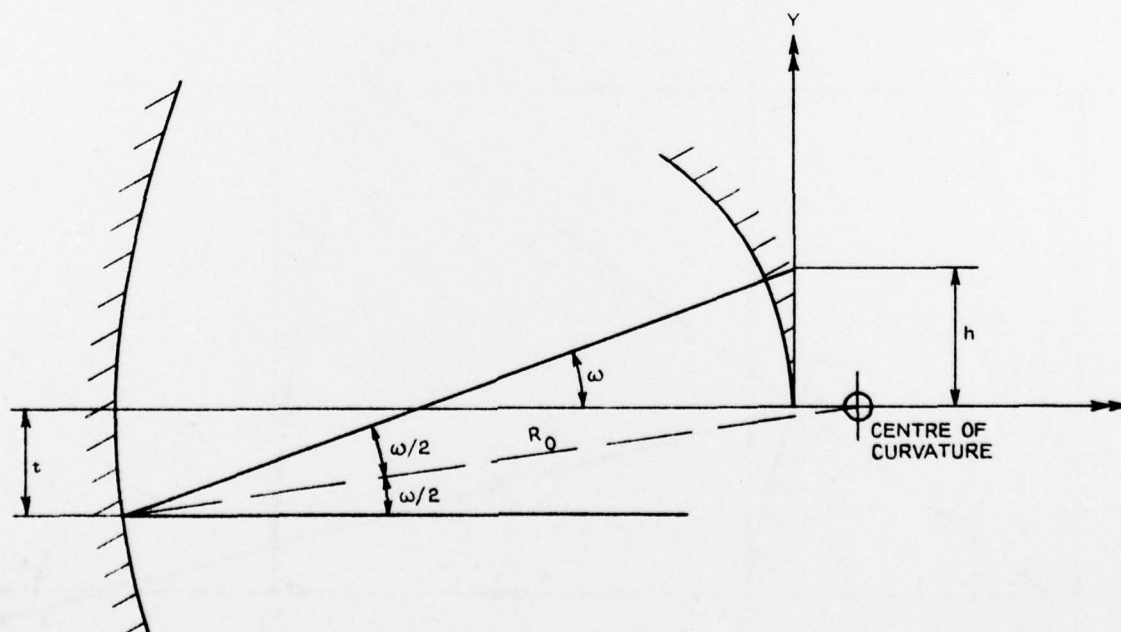


Figure 7. In going congruence sector scanner

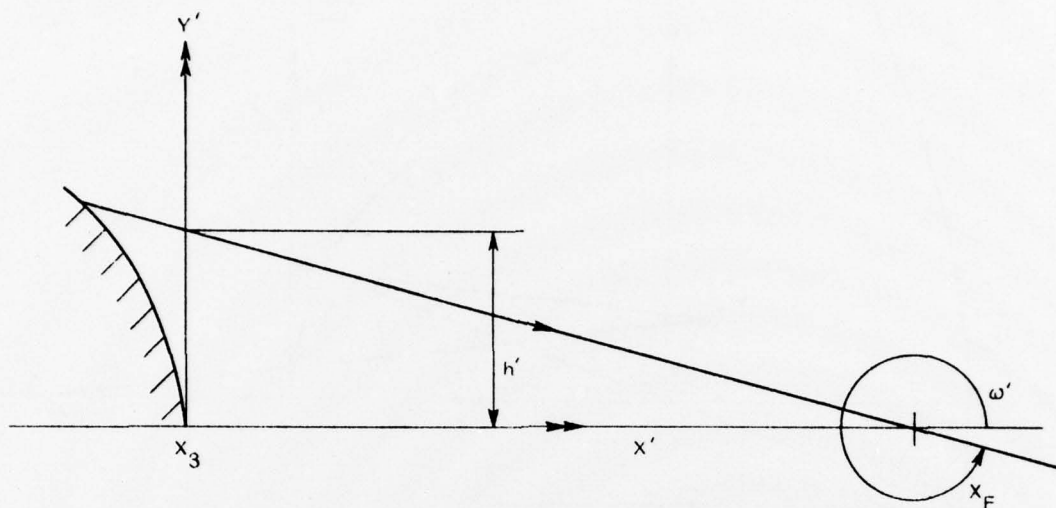


Figure 8. Out going congruence sector scanner

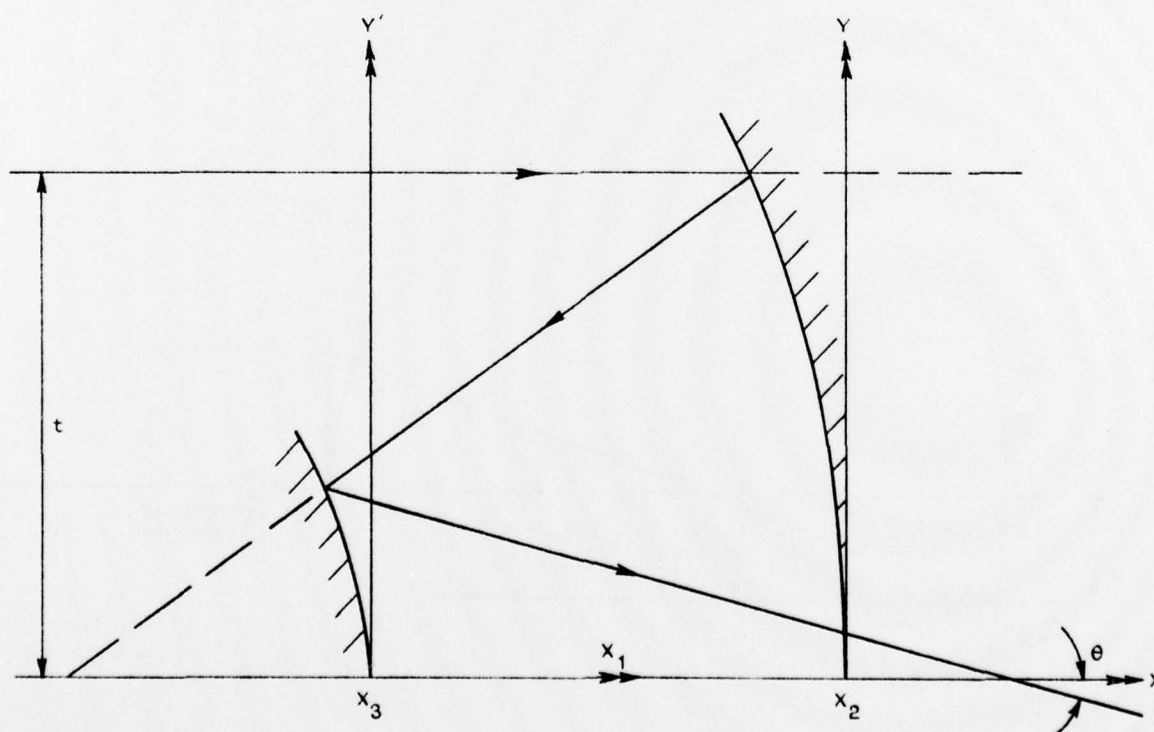


Figure 9. Congruences bolometer radiometer

DISTRIBUTION

EXTERNAL

Copy No.

In United Kingdom

Ministry of Defence, Defence Research Information Centre 1

In United States

Department of Defense, Defense Documentation Center 2 - 13

In Canada

Ministry of Defence, Defence Science Information Service 14

In New Zealand

Ministry of Defence 15

In Australia

Chief Defence Scientist 16

Controller, Programme Planning and Policy Division 17

Executive Controller, Australian Defence Scientific Service 18

Superintendent, Defence Science Administration 19

Assistant Secretary, Defence Information Services
(for microfilming) 20

Defence Library, Campbell Park 21

Library, Aeronautical Research Laboratories 22

Library, Materials Research Laboratories 23

Australian National Library 24

Director, Joint Intelligence Organisation (DDSTI) 25

INTERNAL

Director 26

Chief Superintendent, Applied Physics Wing 27

Superintendent, Optics and Surveillance Division 28

Senior Principal Officer, Optics and Surveillance Division 29

Principal Officer, Night Vision Group 30

Principal Officer, Mechanical and Optical Techniques Group 31

Principal Engineer, Mechanisms and Instrumentation Group 32

Mr N. Bromilow, Mechanical and Optical Techniques Group 33

Mr J. Considine, Mechanism and Instrumentation Group 34

Mr M. Stratton, Mechanism and Instrumentation Group 35

Mr M.R. Meharry, Night Vision Group 36

Mr K.C. Liddiard, Night Vision Group 37

Mr J. Ward, Night Vision Group 38

Mr J. Hlava, Night Vision Group 39

Mr A.R. Jackson, Night Vision Group 40

WRE-TR-1742(A)

Author

W.R.E. Library

Spares

Copy No.

41 - 42

43 - 44

45 - 54